



Synthesis, Characterization, of Novel Pyrazolo [3,4-d] Pyrimidine Derivatives, Via Microwave Irradiation and Study Anti-Tumor Activity by Molecular Docking

WAFAA MAHDI ALKOOFEE^{1*} and ZAINAB Y. KADHIM²

¹Department of Chemistry, College of Sciences/AL-Muthanna University, Samawah, 66001, Iraq.

²Department of Physiology, Pharmacy and Chemistry, College of Veterinary Medicine/AL-Muthanna University, Samawah, 66001, Iraq.

*Corresponding author E-mail: wafamahdi@mu.edu.iq

<http://dx.doi.org/10.13005/ojc/410638>

(Received: November 01, 2025; Accepted: December 23, 2025)

ABSTRACT

Cancer comprises a wide spectrum of disorders characterized by uncontrolled cellular growth and the capacity of cancer cells to infiltrate and damage surrounding tissues. The increasing global incidence of cancer has intensified the search for new therapeutic agents with improved efficacy. In the present work, a new series of heterocyclic derivatives incorporating the structure based on pyrazolo [3,4-d]pyrimidine scaffold was prepared through microwave methodology. The obtained compounds had their chemical structure successfully established and concluded C.H.N, FT-IR, NMR (¹H and ¹³C), and mass spectrometric analyses, in addition to evaluating their physical properties. The anticancer potential of the prepared derivatives was assessed toward the (MCF-7). Breast carcinoma cell line using the MTT assay. Among the compounds, Z₂ displayed the strongest growth-inhibitory effect. Hemolysis testing further revealed low percentages of red blood cell lysis at 10 mg/mL (4.05% for Z₂ and 4.18% for Z₁), indicating that both compounds exhibit acceptable biological safety. The free-radical-scavenging ability of the primed compounds was inspected using the DPPH-based antioxidant assay, and the findings confirmed that Z₂ possesses higher radical-scavenging activity compared with Z₁. Overall, the prepared obtained pyrazolo[3,4-d]pyrimidine-based derivatives exhibited notable anticancer as well as antioxidant properties, suggesting their potential as lead structures for further development.

Keywords: 4-(3-Chloro-4-hydroxy-5-methylphenyl)-3-methyl-1,4,5,7-tetrahydro-6H-pyrazolo[3,4-d]pyrimidine-6-thione(Z₁), 4-(3-(Chloromethyl)-2-hydroxy-5-nitrophenyl)-3-methyl-1,4,5,7-tetrahydro-6H-pyrazolo[3,4-d]pyrimidin-6-one(Z₂). anticancer, Antioxidant DPPH, MCF-7, Fluorescent.

INTRODUCTION

Cancer is recognized as one of the major global health challenges, as its association with uncontrolled cell proliferation and the ability of malignant cells to invade neighboring tissues¹.

Recent statistics indicate that cancer remains the second major reason of mortality globally, responsible for around 9.6 million deaths in 2018². The initiation and progression of cancer are often linked to genetic alterations, disturbances in normal cell differentiation, and exposure to external risk factors



such as certain drugs, smoking, and unhealthy dietary habits³. Among the wide range of heterocyclic systems investigated for anticancer applications, the pyrazolo[3,4-d]pyrimidine framework has attracted considerable research interest⁴. This fused bicyclic system, composed of pyrazole and pyrimidine moieties, has demonstrated versatile biological and pharmacological properties, including antiviral, antibacterial, antidiabetic, antiproliferative, herbicidal, and antioxidant activities^{5,6}. Beyond its biological relevance, the pyrazole ring is also valuable in industrial chemistry and frequently serves as a key precursor for other heterocyclic structures⁷. Pyrimidine-based compounds, in particular, are known for their broad therapeutic potential, acting as anticancer, antibacterial, antifungal, insecticidal, and antiviral activities⁸. Derivatives established on the Pyrazolo[3,4-d]pyrimidine framework illustrate structural similarity to purine systems, which enhances their application in drug design⁹. This resemblance supports their use as adenosine biososteres, enabling them to maintain essential interactions within kinase active sites¹⁰. Protein kinases are implicated in numerous pathological conditions, including cancer, and thus represent important therapeutic targets¹¹. As a result, significant efforts have focused on the development of novel pyrazolo[3,4-d]pyrimidine derivatives exhibiting enhanced inhibitory properties. Several studies have reported that derivatives of this heterocyclic scaffold exhibit notable anticancer activity by suppressing the function of key enzymes such as CDK1, CDK2, and lipoyxygenase¹². Because the heterocyclic pyrazolo[3,4-d]pyrimidine moiety forms part of the core structure for many EGFR-TK inhibitors, it has emerged as a promising pharmacophore in anticancer drug design¹³. Numerous analogues have been evaluated as anticancer agents, and some have received FDA approval¹⁴. Structural investigations have shown that the nitrogen atom adjacent to the aryl substituent at position 4 has a significant influence on biological activity¹⁵. Incorporation of further functional substituents into this scaffold has led to derivatives resulting in pronounced anticancer effects across multiple cancer cell lines¹⁶. Heterocyclic chemistry continues to be a central theme in medicinal chemistry, as most clinically used drugs incorporate heterocyclic components that significantly influence their pharmacological activity¹⁷. Advances in synthetic methodologies have enabled the efficient preparation

of nitrogen-containing heterocyclic, which participate in essential biological functions and serve as key intermediates in the synthesis of pharmacologically important molecules¹⁸. Accordingly, the present study focuses on pyrazolo[3,4-d]pyrimidine derivatives¹⁹, which consist of a five-membered ring heterocycle bearing two nitrogen atoms at positions 1,2 fused with a six-membered pyrimidine ring that includes two additional nitrogen atoms at positions 1 and 3²⁰. Owing to the presence of several reactive sites within this scaffold these molecules exhibit pronounced reactivity toward both electrophilic and nucleophilic reagents²¹. A wide variety of pyrazolo[3,4-d]pyrimidine derivatives have exhibited promising biological properties, including potent anticancer and antioxidant activity²². The present work also incorporates molecular docking investigations aimed at examining the interaction between the synthesized compounds and selected biological targets, providing theoretical support for their observed pharmacological behavior. In recent years, computational methods have become increasingly important in identifying new therapeutic candidates and in optimizing approved drugs through structure-based design²³. Molecular modeling tools provide an efficient platform that bridges computational science with medical research, enabling the rapid evaluation of natural and synthetic compounds through virtual screening approaches²⁴. These techniques offer valuable insights into the possible interactions between drug molecules and biological targets, thus guiding the development of more potent anticancer agents. Given the broad pharmacological potential of pyrazolo[3,4-d]pyrimidine-based composites and their structural compatibility with biologically active systems, the present study aims to synthesize new derivatives of this heterocycle and explore their theoretical affinity toward selected cancer-related enzymes using molecular docking. The study further evaluates the biological performance of the prepared compounds through *in-vitro* anticancer, antioxidant, and hemolysis assays, providing a comprehensive understanding of their therapeutic prospects.

EXPERIMENTAL

Materials and instrumentation

All reagents and chemicals employed throughout this work were obtained from commercial sources, including Sigma-Aldrich, Fluka, and Merck. The human breast cancer cell line (MCF-7) was supplied by the national cell bank of

Iran (Pasteur Institute, Tehran). Antioxidant and cytotoxicity tests were performed at the College of Veterinary Medicine, Al-Muthanna University, where a Panasonic NNST300W microwave oven was also utilized for synthetic procedures. Fourier-transform infrared (FT-IR) spectroscopy and elemental C.H.N analyses were performed at the Department of Chemistry College of Science Al-Muthanna University. proton (^1H) and carbon (^{13}C)NMR spectra, as well as mass spectrometric analyses, were recorded at the University of Tehran, Iran. In addition, theoretical molecular docking studies were carried out using MOE 2015.10 software before initiating the experimental work.

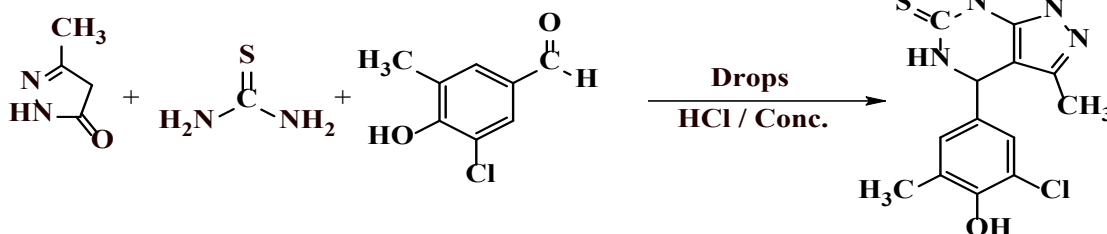
Step-I. General Method for the Prepare of the Pyrazolo[3,4-d]pyrimidine ring via microwave irradiation^{26,27}

The pyrazolo[3,4-d]pyrimidine ring was prepared by mixing equimolar amounts of 3-methyl-2-pyrazolin-5-one (0.01 mol), an appropriate Aromatic Aldehyde (0.01 mol), and thiourea or urea (0.01 mol) in acetonitrile (5 mL). The reaction mixture was magnetically stirred until complete dissolution was formed, after which 3-4 drops of concentrated hydrochloric acid. The reaction system was then subjected to microwave irradiation at 300W for a period of 3-5 min, leading to the gradual formation of a yellow to off-white precipitate. The improvement of the reaction was followed by TLC thin-layer chromatography by use hexane: ethyl acetate (7:3) as the eluent. After completion, the reaction mixture was allowed to cool, after which the solid product was collected by filtration, washed with acetonitrile, and oven-dried. The synthesized derivatives were characterized by melting point determination, TLC behavior, IR, ^1H -NMR, C.H.N elemental analysis, and mass spectra, and comparing the obtained data with

literature values to confirm their structures.

Compound No.(1):4-(3-Chloro-4-hydroxy-5-methylphenyl)-3-methyl-1,4,5,7-tetrahydro-6H-pyrazolo[3,4-d]pyrimidine-6-thione(Z1)

Compound Z1 was synthesized by treating an equimolar mixture of 3-chloro-4-hydroxy-5-methylbenzaldehyde (0.01 mol, 1.70 g), 3-methyl-2-pyrazolin-5-one (0.01 mol, 0.98 g), and thiourea (0.01 mol, 0.76 g) with a catalytic amount of concentration hydrochloric acid. The reaction afforded a yellow solid, melting at 125–127°C, with an isolated yield of 67%. The R_f value is 0.8. Elements analysis for (C₁₃H₁₃ClN₄OS); (M.Wt: 308.78), gave the following results: calculated C, 50.57; H, 4.24; N, 18.14%. Found. C, 50.23; H, 3.89; N, 17.67. FT-IR (KBr, cm⁻¹) spectrum exhibited characteristic absorption bands at: 3381.33 ν (NH-Pyrimidine), 3277.17 (NH-Pyrimidine), 3130.45 (NH-Pyrazole), 3000.09 (Ar-H), 2996.93 (aliphatic C-H), 1666.55 (Pyrazole, C=N), 1616.40 (N-H bending), 1512.24–1469.81 ν (Ar, C=C), 1161.19 (C=S), and 779.27 ν (C-Cl). ^1H -NMR (500 MHz, DMSO-d₆, δ /ppm): δ (s, 2.07 ppm, 3H, Ph-CH), δ (s, 2.26 ppm, 3H, Pyrazole-CH), δ (s, 5.02 ppm, 1H, CH-Pyrimidine), δ (m, 6.76–6.78 ppm, 2H, Ar-H), δ (s, 7.15 ppm, 1H, NH-Pyrazole), δ (s, 7.16 ppm, 1H, NH-Pyrimidine), δ (s, 7.51 ppm, 1H, NH-Pyrimidine), δ (s, 13.45 ppm, 1H, OH). ^{13}C -NMR (δ /ppm): δ (14.56, Pyrazole-CH₃), δ (25.10, Ph-CH), δ (78.89, CH-Pyrimidine), δ (117.04–136.27, Ar-C), δ (137.05, Pyrazole C=N), δ (159.52, NH-C=C-NH), δ (174.44, C=S). MS (m/z): 308.78 (M⁺, R% 23864), showing the important fragmentation peaks at 41 m/z, 50 m/z, 57 m/z, 69 m/z, 98 m/z, 115 m/z, 129 m/z, 144 m/z, 173 m/z, 201 m/z, 265 m/z, and 281 m/z. these spectral results collectively support the successful synthesis of the target compound and are consistent with its proposed structure.



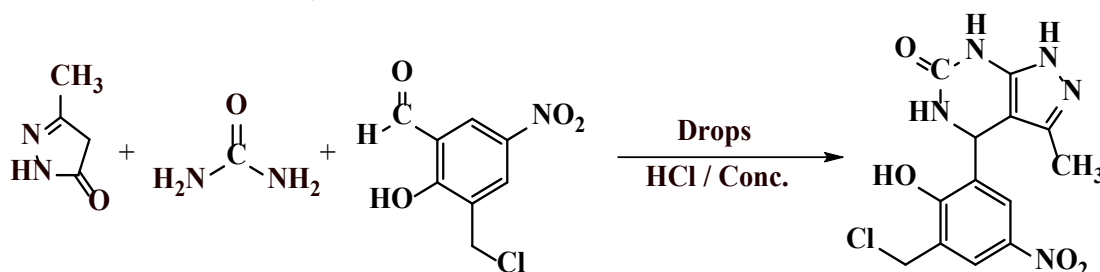
Compound No.(2):4-(3-(Chloromethyl)-2-hydroxy-5-nitrophenyl)-3-methyl-1,4,5,7-tetrahydro-6H-pyrazolo[3,4-d]pyrimidin-6-one(Z2).

Compound (Z2) was prepared by adding

a few drops of concentrated hydrochloric acid to a mixture of 3-(chloromethyl)-2-hydroxy-5-nitrobenzaldehyde (0.01 mol, 2.15 g), 3-methyl-2-pyrazolin-5-one (0.01 mol, 0.98 g), and urea (0.01

mol, 0.60 g). The product is a yellow powder with a melting point of 200–201°C and a yield of 77%. The Rf value is 0.6. Analysis of the elements (C₁₃H₁₂ClN₅O₄); (M.Wt: 337.72). Calc.. C, 46.23; H, 3.58; N, 20.74%. Found. C, 47.01; H, 4.11; N, 21.23. FT-IR (KBr, cm⁻¹): stretching, (OH, aromatic) 3381.33, ν (NH-Pyrimidine) 3277.17, ν (NH-Pyrimidine) 3174.94, ν (NH-Pyrazole) 3160.85, ν (Ar-H, sp²-CH) 3090.67, ν (C-H, aliphatic sp³) 2916.26, ν (C=N, imine) 1693.96, ν (Ar, C=C) 1614.47, ν (C=O) 1672.34, ν (C-Cl) 763.83. ¹H-NMR (500 MHz, DMSO-d₆, δ /ppm): δ (s, 2.25ppm, 3H, Pyrazole-CH), δ (s, 2.69ppm, 2H, CH-Cl), δ (s, 5.11ppm, 1H, CH-Pyrimidine), δ (m, 7.32–

7.50ppm, 2H, Ar-H), δ (s, 8.11ppm, 1H, NH-Pyrazole), δ (s, 8.81ppm, 1H, NH-Pyrimidine), δ (s, 10.19ppm, 1H, NH-Pyrimidine), δ (s, 13.69ppm, 1H, OH). ¹³C-NMR (δ /ppm): δ (14.06, Pyrazole-CH₃), δ (40.22, Cl-CH), δ (61.73, CH-Pyrimidine), δ (123.87–164.29, Ar-C), δ (137.79, Pyrazole C=N), δ (150.22, NH-C=C-NH), δ (166.96, C=O). MS (m/z): 337.72 (M⁺, R% 2000), showing the important fragmentation peaks at 41 m/z, 57 m/z, 69 m/z, 98 m/z, 115 m/z, 144 m/z, 173 m/z, 201 m/z, 265 m/z, and 309 m/z. These results confirm that the compound was successfully synthesized and is consistent with the expected physical, elemental, and spectroscopic properties.



Step-II. The cytotoxicity of the synthesized pyrazolo[3,4-d]pyrimidine derivatives²⁷

Hemolytic activity of the synthesized compounds were assessed at concentrations of 100, 75, 50, and 25 mg/mL, using DMSO as the dissolving medium and human red blood cells (RBCs) as the biological model. Blood was obtained from healthy donors at Al-Hussein Teaching Hospital, Al-Muthanna, and collected in tubes containing an anticoagulant. To prepare the samples, 0.5 mL of whole blood was mixed with 10 mL of Ringer's solution. From each prepared dilution, 0.8 mL was transferred into separate test tubes, and 0.2 mL of the blood–Ringer suspension was added, bringing the final reaction volume to 1 mL. The tubes were then incubated at 37°C for 30 minutes. Following incubation, the samples were centrifuged at 1000 g for 5 min, and the absorbance of the resulting supernatant was recorded at 570 nm using a UV–Vis spectrophotometer. Two controls were used for comparison:

- **Positive control:** distilled water mixed with RBCs (complete hemolysis)
- **Negative control:** DMSO mixed with RBCs (baseline hemolysis)

$$\text{Hemolysis (\%)} = (D - D_0) / (D - D_0) \times 100$$

The percentage of hemolysis was determined using the following equation:

where:

- D = absorbance of the test sample
- D₀ = absorbance of the negative control (DMSO)
- D₁₀₀ = absorbance of positive control (distilled water)

All measurements were carried out in duplicate to ensure precision and reliability.

Step-III. The evaluation of the biological activity of synthesized compounds as antioxidant agents²⁸

Different concentrations (1000, 800, 750, 400, 200, 50, and 12.4ppm), were combined with 2 mL of a freshly prepared DPPH solution (0.004ppm) in methanol. The reaction mixtures were gently mixed to achieve uniformity and subsequently incubated in the dark for 30 minutes. Absorbance were recorded at 517nm. All measurements were performed in duplicate to ensure accuracy. The same procedure was repeated using ascorbic acid (vitamin C) as a optimistic control. The percentage of ability to scavenge free radicals were determined using the equation below:

$$\text{Inhibition \%} = (A(\text{control}) - A(\text{sample})) / A(\text{control}) \times 100$$

Where:

- A (control) = Absorbance of DPPH + solvent (MeOH)
- A (sample) = Absorbance of DPPH + sample (test compound or standard)

Step-VI: Biological Evaluation of the Synthesized Compounds for Anticancer Activity

Cell lines and culture²⁹

The human breast cancer cell line MCF-7 was sourced from Iran's National Cell Bank (Pasteur Institute). Cells were cultured in RPMI-1640 medium (Gibco) enriched with 10% fetal bovine serum (FBS) and a standard antibiotic mixture consisting penicillin 100 U/mL and streptomycin 100 µg/mL. Cultures were maintained at 37°C under a humidified incubator with 5% CO₂. Routine passaging was carried out using trypsin–EDTA, followed by washing with phosphate-buffered saline (PBS). The same media composition and incubation conditions were applied for both three-dimensional cell colony formation and conventional monolayer cultures.

MTT-Based Cytotoxicity Evaluation in MCF-7 Cells³⁰

The cytotoxic effect of the synthesized compounds against MCF-7 breast cancer cells was investigated using an MTT colorimetric method. In brief, confluent cultures of MCF-7 cells were detached using trypsin, collected, and attuned to a seeding density of 1.4×10^4 cells per well. The cell suspension was transferred into 96-well microplates at a volume of approximately 200 µL per well, followed by incubation for 24 h to allow cell adherence. After monolayers were established, the cells were exposed to a range of compound concentrations (100–6.25 µg/mL) and incubated for another 24 h at 37°C in a controlled environment containing 5% CO₂. Following treatment, the medium was gently aspirated to avoid disturbing the cell layer, and 200 µL of freshly prepared MTT reagent (0.5 mg/mL in PBS) was added to each well. The plates were incubated again for 4 h, enabling the formation of formazan crystals within viable cells. Upon completion of the reaction, the MTT-containing medium was removed, and 100 µL of (DMSO) dimethyl sulfoxide was introduced to dissolve the formed formazan crystals. The plates were gently agitated on an orbital shaker at 37°C until full solubilization was achieved. Absorbance

values were measured at 570nm expending an ELISA microplate reader (Model Wave xs2, BioTek, USA). The percentage of viable cells and the half-maximal inhibitory concentration (IC₅₀) for each compound were calculated based on the derived dose–response curves.

Fluorescent Staining (AO/EB)³¹

Fluorescent staining with acridine orange and ethidium bromide was employed to assess cell viability and death patterns. Initially, MCF-7 cells were seeded into 6-well culture plates, and the IC₅₀ concentrations of the tested compounds were applied for following the 24-h exposure to the test compounds, the treated MCF-7 cells were washed carefully with PBS, after which after which an AO/EB staining solution was applied. The stained cells were immediately visualized under a fluorescence microscope (Axioskop 2Plus, Zeiss, Germany). Discrimination between viable and non-viable cells relies on the variation in membrane permeability toward the fluorescent dyes:

- Green-fluorescent cells correspond to living cells that selectively absorb AO.
- Orange-fluorescent cells represent dead cells that uptake EB.
- Cells displaying both green and orange fluorescence indicate early or late apoptotic stages, where partial membrane permeability allows entry of both dyes.

To maintain data accuracy and consistency, five microscopic fields were randomly chosen from each stained slide for imaging and analysis.

Step-V. Molecular Docking of the Synthesized Compounds³³

Two proteins were selected for the docking study: EGFR (PDB ID: 7OM5) and VEGFR-2 (PDB ID: 4ASD) based on previous research and literature reports. The X-ray crystallographic structures of these proteins were obtained from the RCSB Protein Data Bank (PDB). Molecular docking analysis was performed to further clarify the binding affinity and interactions of the synthesized compounds. MOE 2015.10 software was employed to predict the binding modes and affinities of the chemical structures. The crystal structures of the enzymes were retrieved from the Royal Society of Chemistry Bioinformatics Collaboration and the RCSB PDB (<http://www.rcsb.org/>)

pdb) for docking calculations. The downloaded PDB files were preprocessed by removing water molecules and any co-crystallized ligands. MOE 2015.10 was used to draw and optimize the structures of the synthesized pyrazolo[3,4-d]pyrimidine derivatives before docking. The steps involved in the docking procedure are summarized below:

Step 1: Selection from the PDB

The target proteins for docking studies were obtained from the RCSB Protein Data Bank repository.

Step 2: Protein Structure Refinement

Proteins obtained from the PDB cannot be directly used for docking; they must first be refined. Prior to docking, the protein structures were refined by eliminating all water molecules and any bound ligands or co-crystallized compounds, as part of the

standard protein preparation process.

RESULTS AND DISCUSSION

Molecular Docking Study of the Newly Synthesized Pyrazolo[3,4-d]pyrimidine Derivatives^{34,35}

At the initial stage of this study, a theoretical screening was performed for the compounds intended for synthesis using molecular docking to evaluate their potential activity against specific cancer cell lines. The three-dimensional crystal structures of the selected proteins EGFR and VEGFR-2 were obtained from the Protein Data Bank (PDB). The ligands to be docked were prepared in PDB format using ChemDraw Ultra 15.0. Fig. 1 illustrates the two proteins as visualized in MOE 2015.10 after preparation for docking, including the removal of water molecules and refinement of the structures.

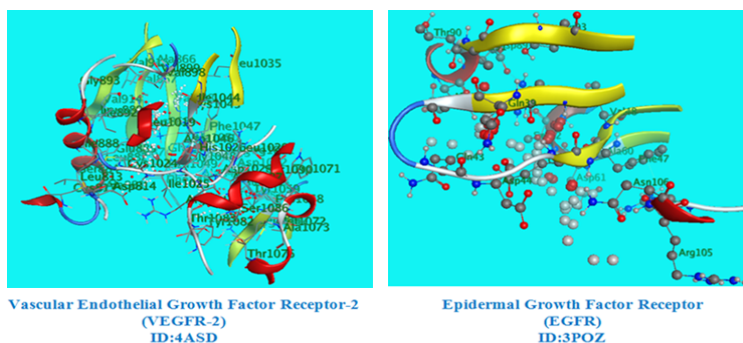


Fig. 1. Displayed on the right is the EGFR structure, whereas the VEGFR-2 structure is presented on the left superior docking results compared to compound (Z_1).

Subsequently, molecular docking studies were carried out using MOE 2015.10. The synthesized pyrazolo[3,4-d]pyrimidine derivatives showed clear interactions within the active sites of both protein targets (7OM5 and 4ASD), indicating promising activity against breast cancer. As presented in Tables (1) and (2), both compounds exhibited notable binding affinities; however, compound (Z_2) demonstrated

Active Site I: 7OM5

The molecular docking results for compound (Z_1) revealed the formation of three hydrogen bonds with the amino acids Arg38, Arg104, and Glu46. The binding energy (G_{bind}) with the EGFR protein was -8.6649 kcal/mol.

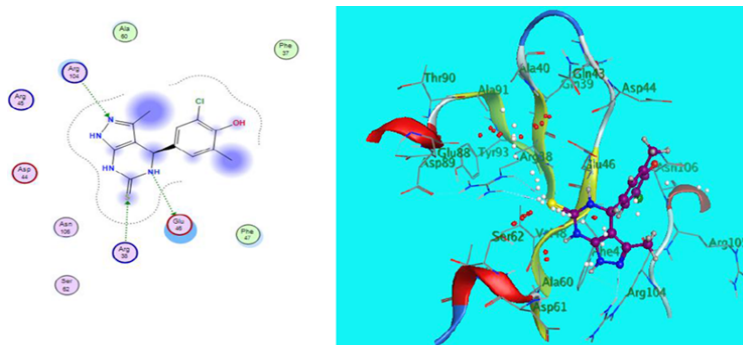


Fig. 2. Three-dimensional and two-dimensional representations of compound (Z_1) docked with the EGFR receptor

The molecular docking results for compound (Z_2) with the same protein demonstrated the formation of two hydrogen

bonds with the amino acids Asp61 and Arg38. The binding energy (ΔG_{bind}) with the EGFR protein was -8.7305 kcal/mol.

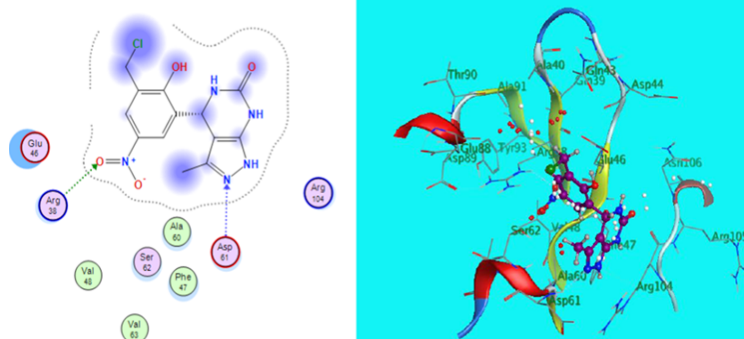


Fig. 3. Three-dimensional and two-dimensional representations of compound (Z_2) docked with the EGFR receptor **Active Site II: 4ASD**

The molecular docking results for compound (Z_1) showed the formation of one hydrogen

bond with the amino acid Asp814. The binding energy (G_{bind}) with the VEGFR-2 protein was -7.9817 kcal/mol.

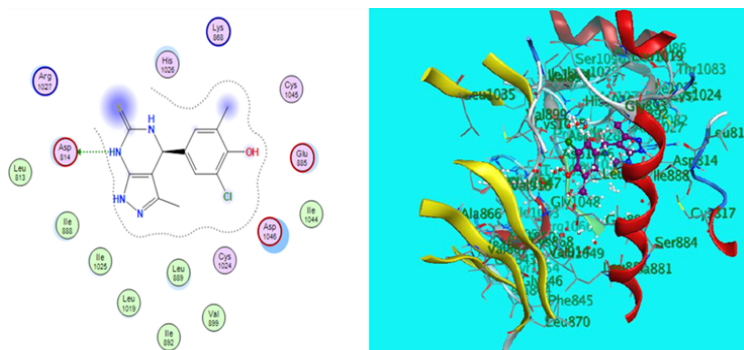


Fig. 4. Three-dimensional and two-dimensional representations of compound (Z_1) docked with the VEGFR-2 receptor

The molecular docking results for compound (Z_2) revealed the formation of four hydrogen bonds with the amino acids Ile1025,

His1026, Glu885, and Asp1046. The binding energy (ΔG_{bind}) with the VEGFR-2 protein was -8.225 kcal/mol.

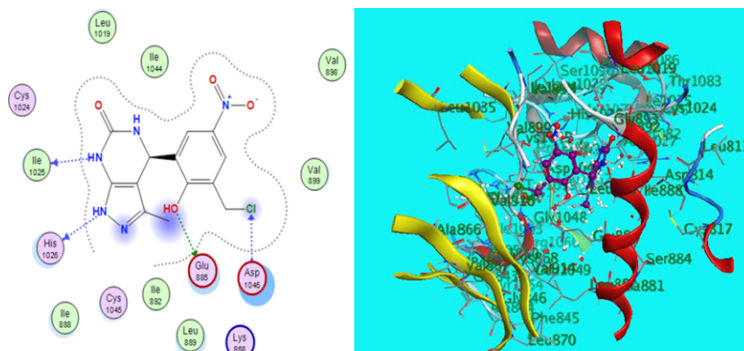


Fig. 5. Three-dimensional and two-dimensional representations of compound (Z_2) docked with the VEGFR-2 receptor

After confirming the theoretical activity of the designed compounds, the heterocyclic derivatives³⁶ containing the pyrazolo[3,4-d]pyrimidine ring were produced and subsequently described using FT-IR, ¹H-NMR, ¹³C-NMR, Mass spectrometry,

and elemental analysis C.H.N.

Evaluation of the Cytotoxicity of the Synthesized Compounds³⁷

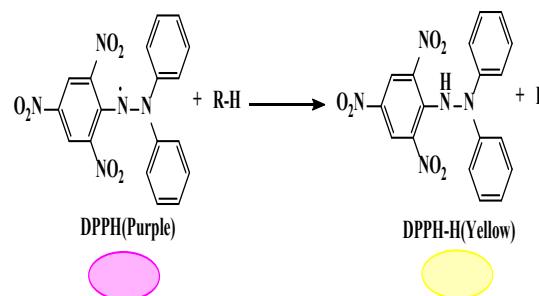
Blood cells were assessed through a

hemolysis assay, which quantitatively measures the amount of hemoglobin released and is considered an important indicator of the potential risk of red blood cell destruction. When the hemolysis percentage is less than 10%, the tested compounds are generally considered safe for intravenous administration. The hemolysis percentages at all tested concentrations were below 5%, as shown in Table 3. At the highest tested concentration (100 mg/mL), the hemolysis percentages were 4.45% for compound (Z₁) and 4.19% for compound (Z₂), respectively. These findings indicate that the synthesized pyrazolo[3,4-d]pyrimidine derivatives are suitable for intravenous administration and exhibit high blood compatibility. The observed cytotoxicity results, obtained by evaluating human red blood cell, confirm that all tested concentrations of the synthesized compounds show no toxic effect on human blood cells. The use of red blood cells in this assay is advantageous because the method is inexpensive, easy to perform, and provides rapid results. This test serves as an essential initial step in determining whether further studies on the compounds should be continued. Red blood cell hemolysis depends on several factors, including compound concentration, incubation time, and temperature. Hemolysis occurs when the cell membrane is disrupted due to interactions between the toxic components of the tested substances and functional groups present in the primary protein structures.

Antioxidant Activity of the Synthesized Compounds³⁸

One of the commonly used methods for evaluating antioxidant activity is the 1,1-diphenyl-2-picrylhydrazyl (DPPH) assay. The antioxidant activity of the synthesized compounds was assessed using the DPPH method according to Blois, which measures the ability of test samples to quench DPPH radicals through hydrogen-donating capacity. Antioxidants convert the DPPH radical into a stable, non-radical molecule through an electron or hydrogen-transfer mechanism. The change in color from purple to yellow indicates an increase in the radical-scavenging activity of the tested compounds. The DPPH radical-scavenging ability was quantified by measuring the decrease in absorbance at 517 nm. It is widely reported that organic compounds containing electron-donating groups (such as amino, methoxy, and hydroxyl groups) can function as potent free-radical scavengers. According to Table 4, all synthesized compounds exhibited good

antioxidant activity when compared with ascorbic acid (standard). At the lowest tested concentration (12.4 µg/mL), the inhibition percentages were 23.49%, 35.67%, and 54.94% for ascorbic acid, Z₁, and Z₂, respectively. At the highest concentration (1000 µg/mL), the compounds showed inhibition values of 96.67%, 87.56%, and 99.77% for ascorbic acid, Z₁, and Z₂, respectively. Compound (Z₂) demonstrated the highest radical-scavenging activity compared to (Z₁). For both Z₁ and Z₂, the OH group on the aromatic ring plays a crucial role in antioxidant activity. The hydroxyl group on the phenyl ring interacts with oxygen radicals to form a semi-quinoid radical, effectively terminating the oxidation chain reaction. Additionally, the π-electrons of the aromatic rings help stabilize electron deficiency and prevent oxidation. Moreover, the presence of N-H and C=O groups in the pyrazolo[3,4-d]pyrimidine scaffold further contributes to the radical-scavenging properties of these compounds.



Scheme 1. Ability to Scavenging DPPH Free Radicals

Anticancer Activity of the Synthesized Compounds Evaluated by the (MTT) Assay³⁹

Obesity represents a major risk factor for a wide range of malignancies, including breast cancer, as it increases the likelihood of disease recurrence and mortality. Extensive research on various metabolic and molecular pathways has successfully established a biological link between obesity and breast cancer. In the present study, the anticancer functional properties of the synthesized compounds (Z₁ and Z₂) were evaluated against the breast cancer cell line MCF-7 by determining their ability to inhibit cell growth (cytotoxicity percentage). The cytotoxic effect of the synthesized pyrazolo[3,4-d]pyrimidine derivatives on MCF-7 cells was assessed, and the IC₅₀ values of the tested compounds were determined accordingly. 1.4-(3-chloro-4 hydroxy-5-methylphenyl)-3-methyl-1,4,5,7-tetrahydro-6H-pyrazolo[3,4-d]pyrimidine-6-thione (Z₁) [IC₅₀=26.20 µg/mL] 2.4-[(3-(chloromethyl)-2-hydroxy-

5-nitrophenyl)-3-methyl-1,4,5,7-tetrahydro-6H-pyrazolo[3,4-d]pyrimidin-6-one(Z₂)[IC₅₀ = 21.04 µg/mL]. The MTT cytotoxicity assay demonstrated that all synthesized compounds exhibited inhibitory activity against MCF-7 breast cancer cells. Based on the obtained data, compound (Z₂) showed the highest inhibitory potency compared to compound (Z₁), which can be attributed to its stronger ability to scavenge free radicals. In contrast, compound (Z₁) displayed comparatively lower cytotoxic activity against the MCF-7 cancer cell line. When compared with the standard anticancer drug Tamoxifen, which exhibited an IC₅₀ = 15.28 µg/mL, both synthesized compounds showed significant activity. Additionally, the compounds were evaluated against normal breast cell lines (MCF-10A) to assess their selectivity and safety profile.

The IC₅₀ values of the synthesized pyrazolo [3,4-d]pyrimidine derivatives were as follows:

1. 4-(3-chloro-4-hydroxy-5-methylphenyl)-3-methyl-1,4,5,7-tetrahydro-6H-pyrazolo[3,4-d]pyrimidin-6-thione (Z₁) IC₅₀ = 52.75 µg/mL
2. 4-(3-(chloromethyl)-2-hydroxy-5-nitrophenyl)-3-methyl-1,4,5,7-tetrahydro-6H-pyrazolo[3,4-d]pyrimidin-6-one (Z₂) IC₅₀ = 35.17 µg/mL

As shown in Table 4 and Fig. 7 and 8, the theoretical results obtained from the molecular docking studies were consistent with the experimental findings.

Anticancer Activity of the Synthesized Compounds Evaluated by Fluorescence Microscopy⁴⁰

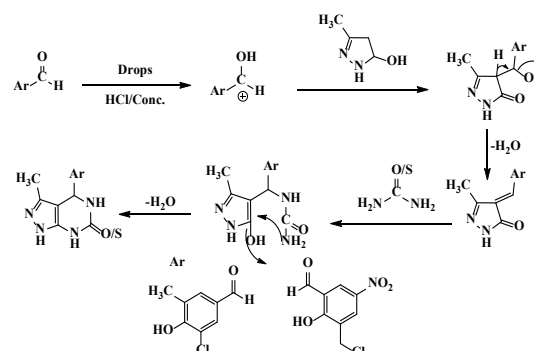
To distinguish between live and dead cells, an additional approach was employed in this study using AO/EB fluorescent staining. MCF-7 cells were seeded into 6-well culture plates, and the IC₅₀

concentrations of the synthesized compounds were applied for 24 hours. After treatment, the cells were washed with double PBS, allowing visualization of nuclear changes and apoptotic body formation characteristic of apoptosis progression. Due to differences in membrane permeability, both live and dead cells become stained.

The AO/EB staining technique allows clear differentiation of cell states:

- Live cells appear uniformly green (AO only),
- Dead cells appear orange (EB uptake),
- Early and late apoptotic cells display combined green and orange fluorescence.

In this study, the cytotoxic effects of the synthesized compounds (Z₁ and Z₂) on the human breast cancer cell line MCF-7 were evaluated and compared. The MTT assay indicated that the presence of functional groups (Cl, OH, CH₂, NO₂) in compound (Z₂) enhances its cytotoxic activity (lower IC₅₀) compared to compound (Z₁), which contains (Cl, OH, CH₂) as functional groups. This structural variation contributes to the increased apoptotic cell death observed with compound (Z₂).



Scheme 2. Reaction Mechanism of the Synthesized Compounds^{41,42}

Molecular Docking Evaluation of the Synthesized Compounds:

Table 1: Docking results of the interaction of the synthesized compounds with the epidermal growth factor receptor (EGFR)

Proteins	ID	Comp.	E _{Binding} Kcal/mol	rmsd-refine	Bonding	Interaction	Distance	Kcal/mol
Epidermal Growth Factor Receptor (EGFR)	7OM5	Z ₁	-8.6649	1.5264	GLU46:OE1/LIG:N	H-donor	3.25	-0.9
					ARG104:NH1/LIG:N	H-acceptor	3.27	-3.1
					ARG38:NH2/LIG:S	H-acceptor	4.40	-3.2
Epidermal Growth Factor Receptor (EGFR)	7OM5	Z ₂	-8.7305	1.9644	ASP61:N/LIG:N	H-acceptor	3.28	-1.7
					ARG38:NE/LIG:O	H-acceptor	2.91	-0.8

Table 2 Docking analysis of the synthesized compounds against the VEGFR-2 receptor.

Proteins	ID	Comp.	EBinding Kcal/mol	rmsd-refine	Bonding	Interaction	Distance	Kcal/mol
Vascular Endothelial Growth Factor Receptor-2 (VEGFR-2)	4ASD	Z1	-7.9817	1.1758	ASP814:OD2/LIG:N	H-donor	2.87	-2.5
Vascular Endothelial Growth Factor Receptor-2 (VEGFR-2)	4ASD	Z2	-8.2253	1.4065	ILE1025:O/LIG:N HIS1026:O/LIG:N	H-donor H-donor	2.93 2.86	-3.4 -5.4
				GLU885:OE2/LIG:O ASP1046:N/LIG:Cl	H-donor H-acceptor	2.81 3.28	-2.1 -1.0	

Table 3: Results of the cytotoxicity assay for the synthesized compounds

No	Compound code	HR (%)			
		(25 mg/mL)	(50 mg/mL)	(75 mg/mL)	(100 mg/mL)
1	Z ₁	0.78 %	1.89 %	2.98 %	4.45 %
2	Z ₂	0.67 %	1.57 %	2.85 %	4.19 %

Cytotoxicity of the Synthesized Compounds:

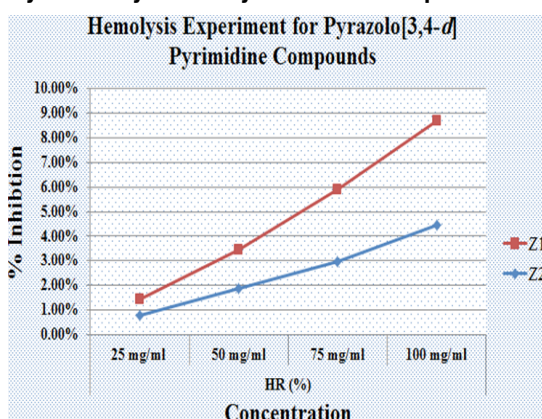


Fig. 6. Hemolytic activity of the synthesized compounds against human red blood cells at different concentrations

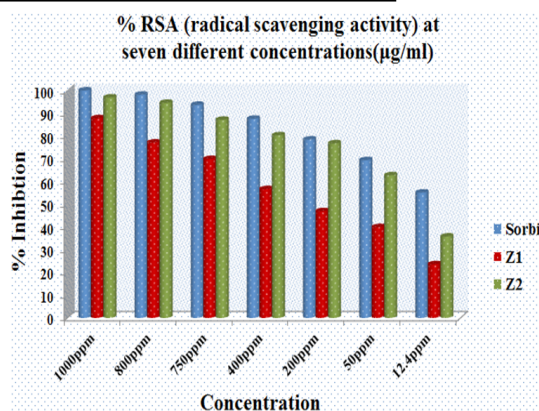


Fig. 7. The synthesized compounds at different conc. compared with ascorbic acid

Anticancer Activity of the Synthesized Compounds

Table 4: Antioxidant Activity of the Synthesized Compounds

No	Compound code	%RSA (radical scavenging activity) at seven different concentrations(µg/mL)						
		1000ppm	800ppm	750ppm	400ppm	200ppm	50ppm	12.4ppm
1	Z1	87.56	76.89	69.67	56.45	46.78	39.78	23.49
2	Z2	96.67	94.34	86.89	80.09	76.56	62.56	35.67
3	Sorbic	99.77	97.89	93.45	87.34	78.23	69.16	54.94

Table 5: Growth inhibition results of MCF-7 breast cancer cells at different concentrations of the synthesized compounds

(Z ₁)IC ₅₀ = 26.20 µg/mL										
Concentration (µg/mL)	6.25	12.5	25	50	100					
absorption at 570 nm	0.551	0.666	0.610	0.503	0.325	0.475	0.096	0.114	0.073	0.098
Viability (%)	80.09	96.80	88.66	73.11	47.24	69.04	13.95	20.93	10.61	14.24
Average Viability (%)	88.44	80.89	58.14	17.44	12.43					
Standard Deviation (±)	11.82	11.00	15.42	4.93	2.57					
(Z ₂)IC ₅₀ = 21.04 µg/mL										
Concentration (µg/mL)	6.25	12.5a	25	50	100					
absorption at 570 nm	0.521	0.504	0.339	0.364	0.303	0.238	0.227	0.228	0.115	0.105
Viability (%)	81.28	78.63	52.89	56.79	47.27	37.13	35.41	35.57	24.18	16.38
Average Viability (%)	79.95	54.84	42.20	35.49	20.28					
Standard Deviation (±)	1.88	2.76	7.17	0.11	5.52					

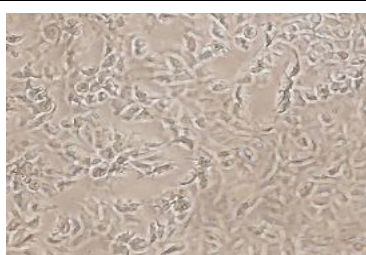
Table 6: Growth inhibition results of normal breast cell lines (MCF-10A) at different concentrations of the synthesized compounds

(Z ₁) IC ₅₀ = 52.75 µg/mL										
Concentration (µg/mL)	6.25	12.5	25	50	100					
absorption at 570 nm	0.606	0.677	0.526	0.674	0.583	0.577	0.400	0.381	0.151	0.150
Viability (%)	88.08	98.40	76.45	97.97	84.74	83.87	58.14	55.38	21.95	21.80
Average Viability (%)	93.24	87.21	84.30	56.76	21.88					
Standard Deviation (±)	7.30	15.21	0.62	1.95	0.10					

(Z ₂) IC ₅₀ = 35.17 µg/mL										
Concentration (µg/mL)	6.25	12.5	25	50	100					
absorption at 570 nm	0.667	0.670	0.473	0.362	0.371	0.415	0.410	0.282	0.074	0.250
Viability (%)	96.95	97.38	68.75	52.62	53.92	60.32	59.59	40.99	10.76	36.34
Average Viability (%)	97.17	60.68	57.12	50.29	23.55					
Standard Deviation (±)	0.31	11.41	4.52	13.16	18.09					



(A). MCF-7 cell lines treated with DMSO



(B). MCF-7 cell lines treated with Z₁ inhibition activity 6.25µg/mL



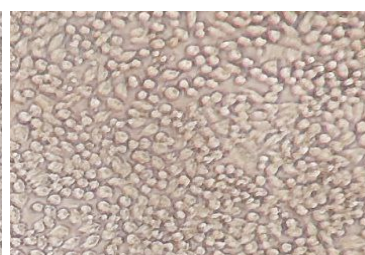
(C). Z₁ inhibition activity 12.5µg/mL



(D). Z₁ inhibition activity 25µg/mL



(E). Z₁ inhibition activity 50 µg/mL



(F). Z₁ inhibition activity 100 µg/mL



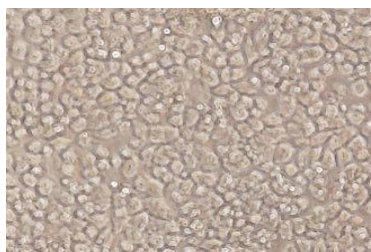
(A). MCF-7 cell lines treated with DMSO



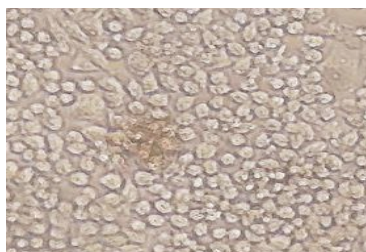
(B). MCF-7 cell lines treated with Z₂ inhibition activity 6.25µg/mL



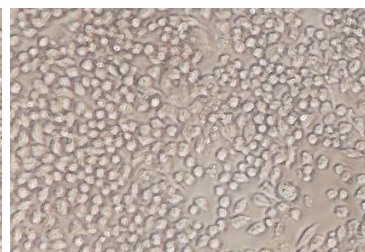
(C). Z₂ inhibition activity 12.5µg/mL



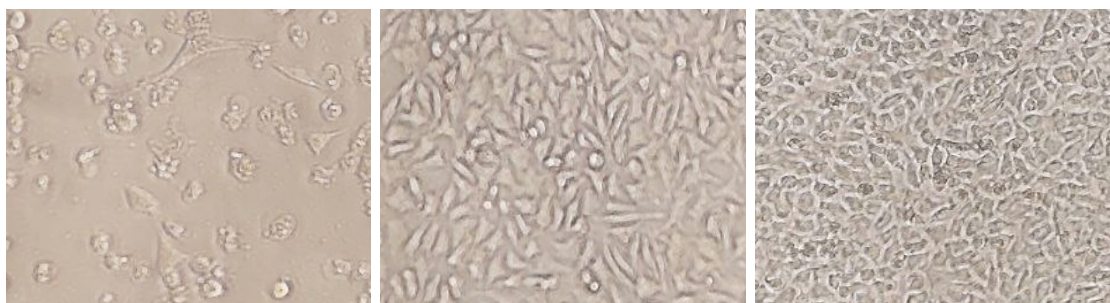
(D). Z₂ inhibition activity 25 25µg/mL



(E). Z₂ inhibition activity 50µg/mL



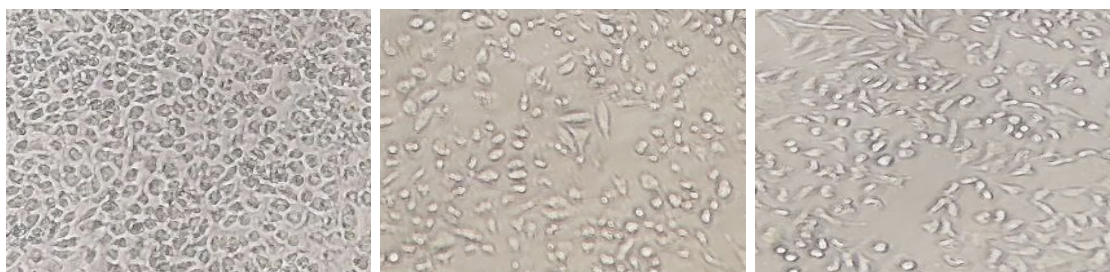
(F). Z₂ inhibition activity 100µg/mL



(A). MCF-10A cell lines treated with DMSO

(B). Z₁ inhibition activity 6.25µg/mL

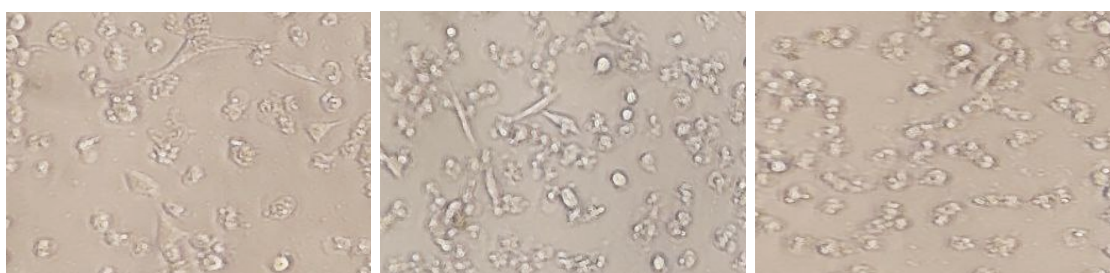
(C). Z₁ inhibition activity 12.5µg/mL



(D). Z₁ inhibition activity 25µg/mL

(E). Z₁ inhibition activity 50µg/mL

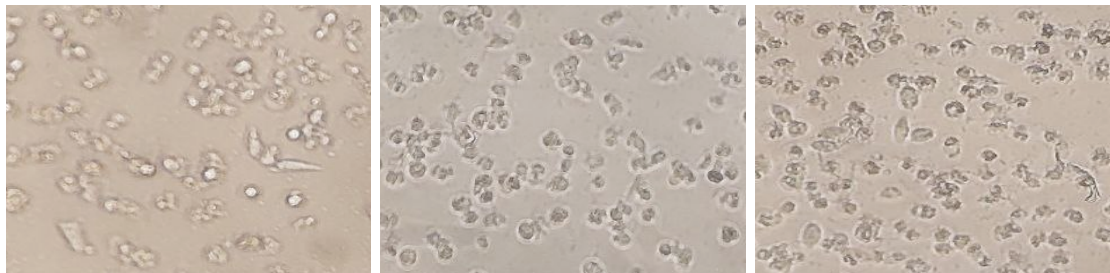
(F). Z₁ inhibition activity 100µg/mL



(A). MCF-10A cell lines treated with DMSO

(B). Z₂ inhibition activity 6.25µg/mL

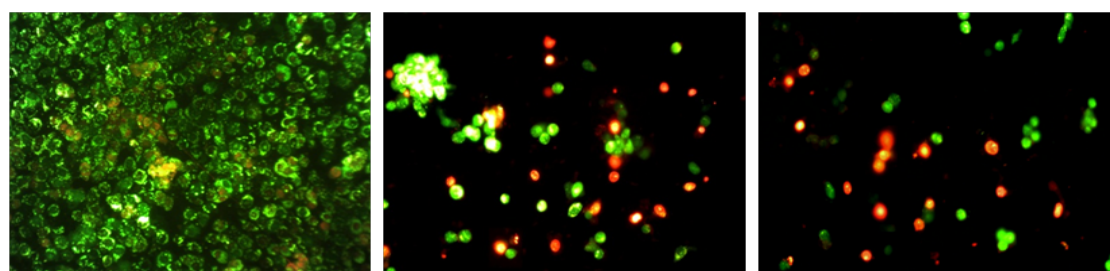
(C). Z₂ inhibition activity 12.5µg/mL



(D). Z₂ inhibition activity 25µg/mL

(E). Z₂ inhibition activity 50µg/mL

(F). Z₂ inhibition activity 100µg/mL



(A). Fluorescence microscopy evaluate the apoptotic effects of comp. (Control)

(B). The apoptotic effects of comp. (Z₁) the cells were exposed with conc. of 6.25µg/mL)

(C). The apoptotic effects of compound (Z₁) the cells were treated with conc. of 12.5µg/mL

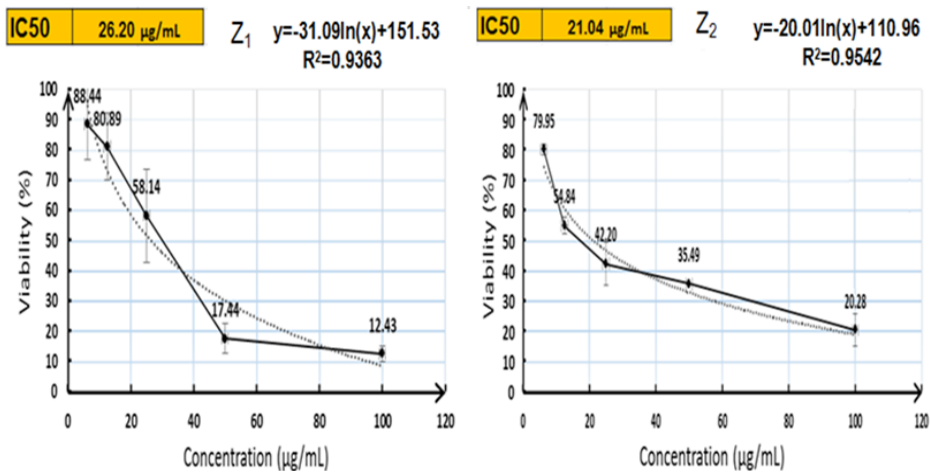
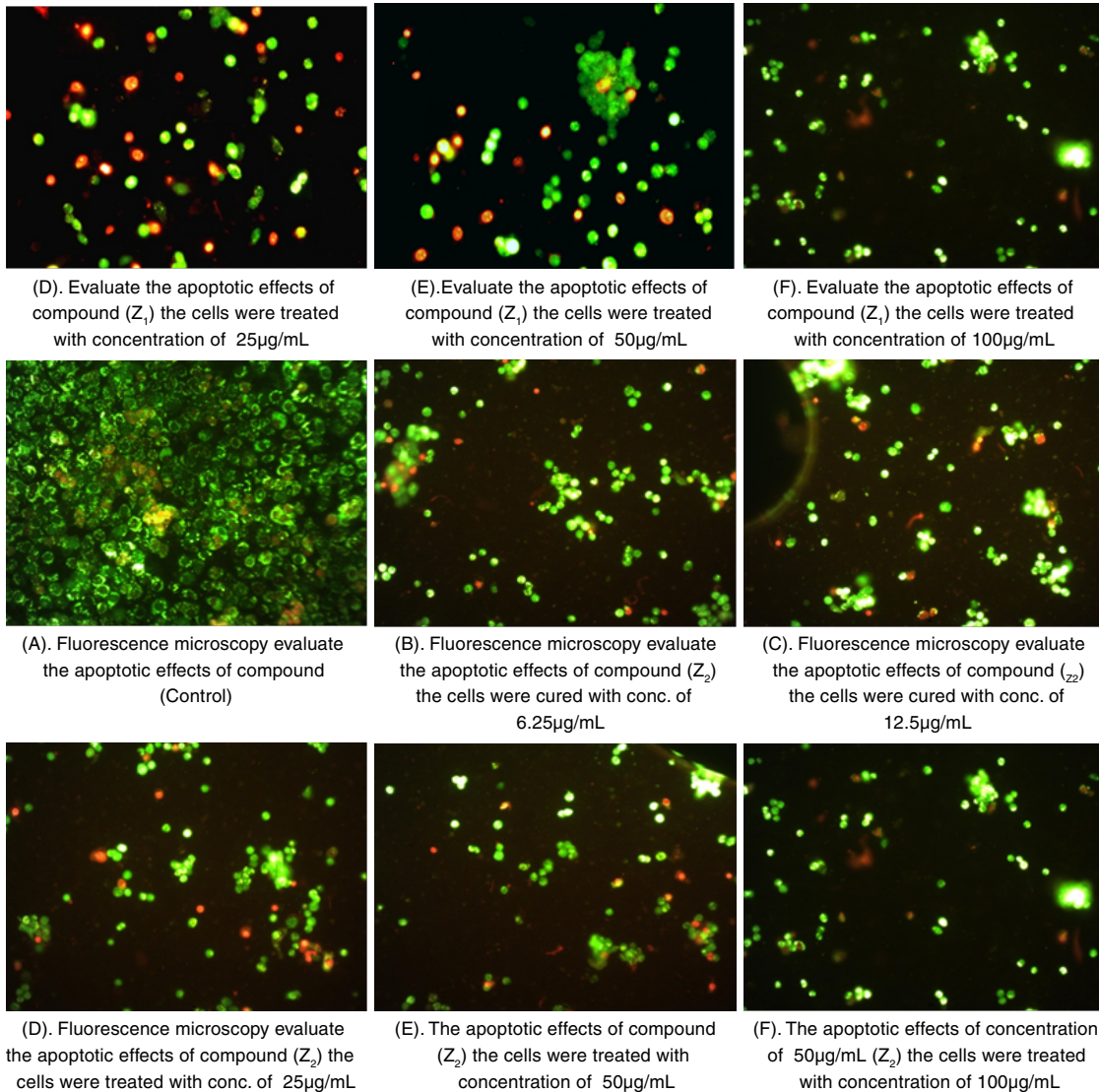


Fig. 8. Antiproliferative activity of MCF-7 breast cancer cells treated with different concentrations of compounds (Z₁ & Z₂)

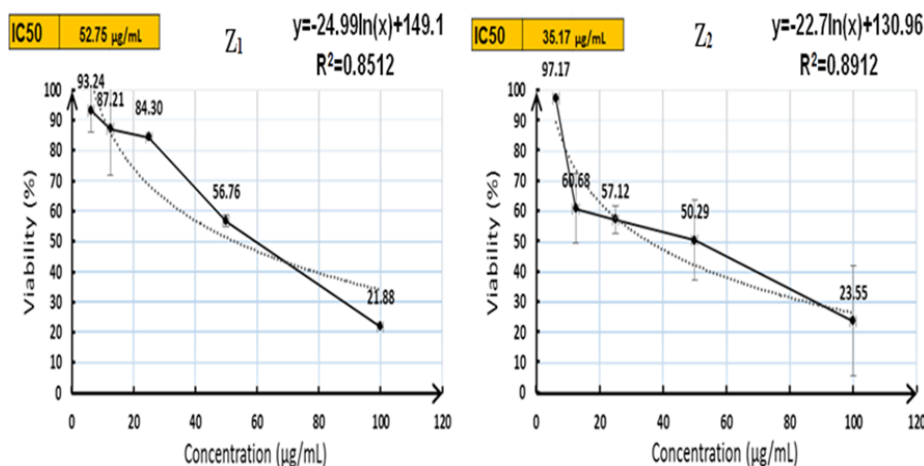


Fig. 9. Antiproliferative activity of compounds (Z_1 & Z_2)

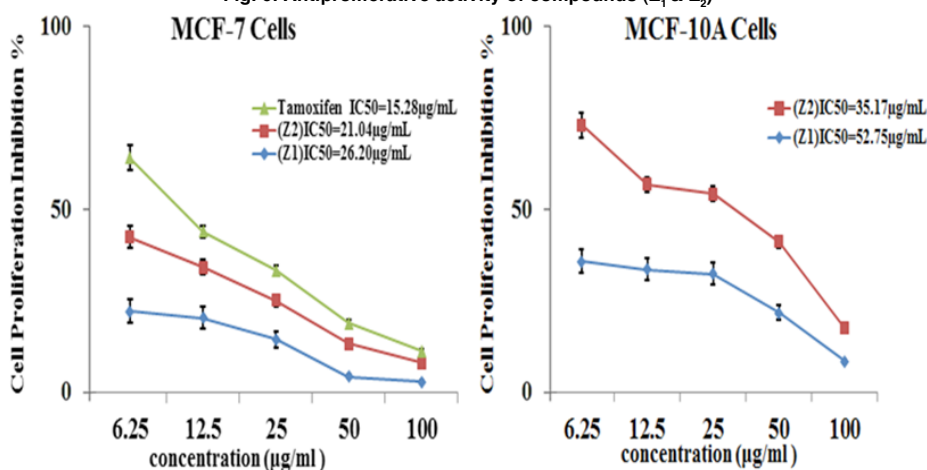


Fig. 10. Antiproliferative activity in MCF-7 breast cancer cells and MCF-10A normal breast cells treated with different concentrations of compounds (Z_1 & Z_2)

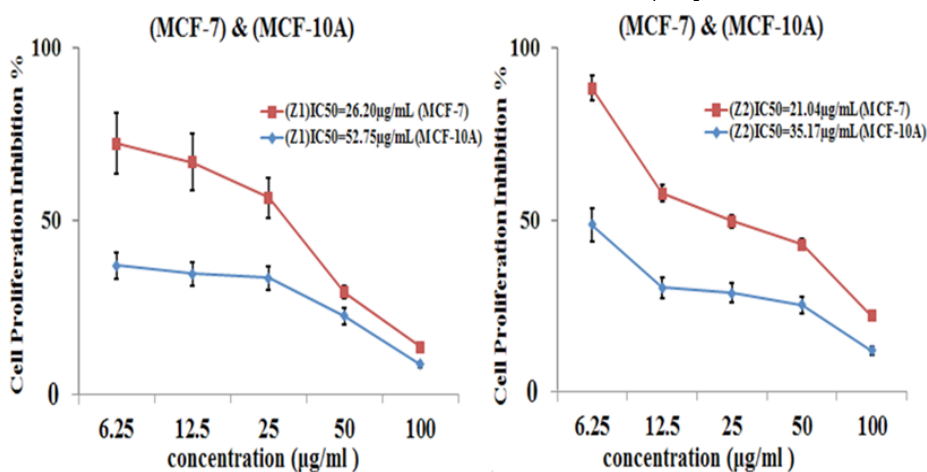


Fig. 11. Comparing the chemicals antiproliferative activity (Z_1 & Z_2)

CONCLUSION

In this study, a series of new pyrazolo[3,4-d]

pyrimidine derivatives were successfully synthesized using simple, low-cost, and environmentally friendly methods that yielded high selectivity and excellent

product purity without generating harmful waste. The structures of the synthesized compounds were thoroughly characterized through multiple analytical techniques FT-IR, ¹H-NMR, ¹³C-NMR, and mass spectrometry, and elemental analysis, confirming their structural integrity and stability under normal environmental conditions. Biological evaluations demonstrated that all synthesized derivatives exhibited high blood compatibility, with hemolysis percentages below the acceptable limit, indicating their safety for potential intravenous administration. Antioxidant assays revealed significant free radical scavenging activity for all compounds, with compound Z₂ showing superior performance. Furthermore, cytotoxicity studies using the MCF-7 breast cancer cell line confirmed that the compounds possess promising anticancer properties, where Z₂ displayed stronger inhibitory effects than Z₁, which aligns with the theoretical predictions obtained from molecular docking studies. Docking results showed favorable binding interactions with key cancer-related protein targets (EGFR and VEGFR-2), further supporting the potential of these derivatives as anticancer agents. Overall, the synthesized pyrazolo[3,4-d]pyrimidine derivatives particularly Z₂ demonstrated strong antioxidant and anticancer activities, suggesting

that they may serve as promising lead compounds for future drug development against breast cancer. Schemes, Figures, and Tables:

ACKNOWLEDGEMENT

The authors would like to acknowledge the College of Science, Al-Muthanna University and the College of Veterinary Medicine, for their partial support and assistance during the course of this research.

Availability of Information and Data

Confirmation to the authors. The findings of the study, and the data supporting it, are given in the paper and its appendices.

Funding

The authors declare that they did not receive any financial support from public, commercial, or non-profit funding agencies for this research.

Conflict of Interest

The authors declare that there is no conflict of interest regarding the publication of this article.

REFERENCE

- Martel, C.; Georges, D.; Bray, F.; Ferlay, J.; & Clifford, G.M., "Global burden of cancer attributable to infections in 2018: a worldwide incidence analysis". *Lancet Glob Health.*, **2020**, *8*(2), e180-e190. DOI: 10.1016/S2214-109X(19)30488-7
- Fragomeni, S.M.; Sciallis, A., & Jeruss, J.S., "Molecular Subtypes and Local-Regional Control of Breast Cancer"., *Surg Oncol Clin N Am.*, **2018**, *27*(1), 95-120. DOI: 10.1016/j.soc.2017.08.005
- Abdel-Megid, M., "Utilities of active methylene compounds and heterocycles bearing active methyl or having an active methine in the formation of bioactive pyrazoles and pyrazolopyrimidines"., *Synth. Commun.*, **2020**, *50*(23), 3563-3591. DOI: 10.1080/00397911.2020.1807570
- Greco, C.; Catania, R.; Balacco, D.L.; Taresco, V.; Musumeci, F.; Alexander, C.; Huett, A., & Schenone, S., "Synthesis and Antibacterial Evaluation of New Pyrazolo[3,4-d]pyrimidines Kinase Inhibitors"., *Molecules.*, **2020**, *25*(22), 5354-5369. DOI:10.3390/molecules25225354
- Kostic, A.; Jovanovic Stojanov, S.; Podolski Renic, A.; Nesovic, M.; Dragoj, M.; Nikolic, I.; Tasic, G.; Schenone, S.; Pes'ic, M., & Dinic, J., "Pyrazolo[3,4-d]pyrimidine Tyrosine Kinase Inhibitors Induce Oxidative Stress in Patient-Derived Glioblastoma Cells"., *Brain Sci.*, **2021**, *11*(7), 884-898. DOI: 10.3390/brainsci11070884
- Kulkarni, R.; Kompalli, K.; Gaddam, N.; Mangannavar, C.V.; Darna, B.; Garlapati, A.; Kumar, D., & Machha, B., "Synthesis, characterization, antitubercular and anti-inflammatory activity of new pyrazolo[3,4-d]pyrimidines"., *Comb. Chem. High Through. Screen.*, **2021**, *24*(8), 1300-1308. DOI: 10.2174/1386207323999200918114905
- Husain, K.; Musad, E., & Hassan, I., "Synthesis, Antibacterial, and Antifungal Evaluation of New Class of Pyrimido[4,5-d]pyrimidine, Pyrazolo[3,4-d]pyrimidine, and Pyrimido[4,5-b]quinoline Derived from α,α -Ketene Dithioacetals as fused Five and Six-membered Heterocycle Derivatives"., *Russian Journal of Bioorganic Chemistry.*, **2023**, *49*(6), 1367-1380. DOI:10.1134/S1068162023060171

8. Li, X.; Li, Z.; Wu, X.; Xiong, Z.; Yang, T.; Fu, Z.; Liu, X.; Tan, X.; Zhong, F., & Wan, X., "Deep Learning Enhancing Kinome-Wide Polypharmacology Profiling: Model Construction and Experiment Validation", *J. Med. Chem.*, **2020**, *63*(16), 8723-8737. DOI: <https://doi.org/10.1021/acs.jmedchem.9b00855>
9. Ambjørner, S.E.B.; Wiese, M.; Köhler, S.C.; Svindt, J.; Lund, X.; Gajhede, M.; Saaby, L.; & Brodin, B., "The pyrazolo[3,4-d]pyrimidine derivative, SCO-201, reverses multidrug resistance mediated by ABCG2/BCRP", *Cells*, **2020**, *4*,9(3), 613, 1-22. DOI: 10.3390/cells9030613
10. Almeahmadi, S.J.; Alsaedi, A.M.R.; Harras, M.F., & Farghaly, T.A., "Synthesis of a new series of pyrazolo[1,5-a]pyrimidines as CDK2 inhibitors and antileukemia", *Bioorganic Chem.*, **2021**, *117*, 105431. DOI: <https://doi.org/10.1016/j.bioorg.2021.105431>
11. Husseiny, E.M., "Synthesis, cytotoxicity of some pyrazoles and pyrazolo[1,5-a]pyrimidines bearing benzothiazole moiety and investigation of their mechanism of action", *Bioorganic Chem.*, **2020**, *102*, 104053. DOI: <https://doi.org/10.1016/j.bioorg.2020.104053>
12. Abdellatif, K.R.A., & Bakr, R.B. "Pyrimidine and fused pyrimidine derivatives as promising protein kinase inhibitors for cancer treatment", *Med. Chem. Res.*, **2021**, *30*(1), 1-19. DOI:10.1007/s00044-020-02656-8
13. Le, X.; Nilsson, M.; Goldman, J.; Reck, M.; Nakagawa, K.; Kato, T.; Ares, L.P.; Frimodt-Moller, B., Wolff, K., & Visseren-Grul, C., "Dual EGFR-VEGF Pathway Inhibition: A Promising Strategy for Patients With EGFR-Mutant NSCLC", *J. Thorac. Oncol.*, **2021**, *16*(2), 205-215. DOI: 10.1016/j.jtho.2020.10.006
14. Omar, A.M.; Ihmaid, S.; Habib, E.S.E.; Althagfan, S.S.; Ahmed, S.; Abulkhair, H.S., & Ahmed, H.E., "The Rational Design, Synthesis, and Antimicrobial Investigation of 2-Amino-4-Methylthiazole Analogues Inhibitors of GlcN-6-P Synthase", *Bioorganic Chem.*, **2020**, *99*, 103781. DOI: <https://doi.org/10.1016/j.bioorg.2020.103781>
15. Ahmed, H.E.; El-Nassag, M.A.; Hassan, A.H.; Mohamed, H.M.; Halawa, A.H.; Okasha, R.M.; Ihmaid, S.; El-Gilil, S.M. A.; Khattab, E.S., & Fouda, A.M., "Developing lipophilic aromatic halogenated fused systems with specific ring orientations, leading to potent anticancer analogs and targeting the c-Src Kinase enzyme", *J. Mol. Struct.*, **2019**, *1186*(15), 212-223. DOI: <https://doi.org/10.1016/j.molstruc.2019.03.012>
16. Rezki, N.; Almeahmadi, M.A.; Ihmaid, S.; Shehata, A.M.; Omar, A.M.; Ahmed, H.E., & Aouad, M.R. "Novel scaffold hopping of potent benzothiazole and isatin analogues linked to 1,2,3-triazole fragment that mimic quinazoline epidermal growth factor receptor inhibitors: Synthesis, antitumor and mechanistic analyses", *Bioorganic Chem.*, **2020**, *103*, 104133. DOI: <https://doi.org/10.1016/j.bioorg.2020.104133>
17. Kassab, A.E.; El Dash, Y., & Gedawy, E.M., "Novel pyrazolopyrimidine urea derivatives: Synthesis, antiproliferative activity, VEGFR-2 inhibition, and effects on the cell cycle profile", *Arch Pharm.*, **2020**, *353*, e1900319. DOI: <https://doi.org/10.1002/ardp.201900319>
18. Lei, T.; Hong, Y.; Chang, X.; Zhang, Z.; Liu, X.; Hu, M.; Huang, W., & Yang, H., "Discovery of the Potent Phosphoinositide 3-Kinase (PI3K) Inhibitors", *Chemistry Select.*, **2020**, *5*, 196-200. DOI: <https://doi.org/10.1002/slct.201904402>
19. Vestri, A.; Pearce, A.K.; Cavanagh, R.; Styliari, I.D.; Sanders, C.; Couturaud, B.; Schenone, S.; Taresco, V.; Jakobsen, R.R.; Howdle, S.M.; Musumeci, F., & Sagnelli, D., "Starch/Poly(glycerol adipate) (Nanocomposites: A Novel Oral Drug Delivery Device", *Coatings*, **2020**, *10*(2), 125. DOI: <https://doi.org/10.3390/coatings10020125>
20. Bailey, J.J.; Jaworski, C.; Tung, D.; Wängler, C.; Wängler, B., & Schirrmacher, R., "Tropomyosin receptor kinase inhibitors: an updated patent review for 2016-2019", *Expert Opinion on Therapeutic Patents.*, **2020**, *30*, 325-339. DOI: <https://doi.org/10.1080/13543776.2020.1737011>
21. Valero, T.; Baillache, D.J.; Fraser, C.; Myers, S.H., & Unciti-Broceta, A., "Pyrazolopyrimidine library screening in glioma cells discovers highly potent antiproliferative leads that target the PI3K/mTOR pathway", *Bioorganic & Medicinal Chemistry.*, **2020**, *28*, 115215. DOI: <https://doi.org/10.1016/j.bmc.2019.115215>

22. Mansour, E.; Aboelnaga, A.; Nassar, E.M.; & Elewa, S.I., "A new series of thiazolyl pyrazoline derivatives linked to benzo[1,3]dioxole moiety: Synthesis and evaluation of antimicrobial and anti-proliferative activities"., *Synthetic Communications*, **2020**, *49*, 368-379. DOI: <https://doi.org/10.1080/00397911.2019.1695839>
23. Joshi, P.; Kawade, V.; Dhulap, S., & Goel, M., "Unlocking the concealed targets using system biology mapping for Alzheimer's disease"., *Pharmacological Reports*, **2019**, *71*, 1104-1107. DOI: <https://doi.org/10.1016/j.pharep.2019.06.012>
24. Dweedat, H.; Mahrous, H.; Sorour, N.; El Ghany, K.A., & Aziz, H.A., "Synthesis, Molecular Docking Studies and ADME Properties of Some New Pyrazolo[1,5-a]pyrimidines as Antimicrobial, and Anticancer Agents"., *Egyptian Journal of Chemistry*, **2024**, *67*(6), 307-316. DOI: [10.21608/EJCHEM.2023.246672.8840](https://doi.org/10.21608/EJCHEM.2023.246672.8840)
25. Adhikari, A.; Bhakta, S., & Ghosh, T., "Microwave-assisted synthesis of bioactive heterocycles: An overview"., *Tetrahedron*, **2022**, *126*(5), 133085. DOI: <https://doi.org/10.1016/j.tet.2022.133085>
26. Ehsanfar, M.; Mosslemin, M.H., & Hassanabadi, A., "A simple and efficient one-pot route for the synthesis of 7-aryl-1,7a-dimethyl-2-phenyl-5-selenoxo-1,2,5,7a-tetrahydro-3H-pyrazolo[3,4-d]pyrimidin-3-ones"., *Phosphorus Sulfur Silicon and Related Elements*, **2020**, *10*(180), 1027-1030. DOI: <https://doi.org/10.1080/10426507.2020.1799211>
28. Alqaraghuli HG.; Kadhim Z.Y., & Seewana, A.N., "Synthesis, Characterization, Theoretical Study, Antioxidant Activity and in Vitro Cytotoxicity Study of Novel Formazan Derivatives Toward MCF-7 Cells"., *Egypt. J. Chem.*, **2022**, *6*(65), 181-188. DOI: [10.21608/EJCHEM.2021.100236.4659](https://doi.org/10.21608/EJCHEM.2021.100236.4659)
29. Kumara, K.; Prabhudeva, M.G.; Vagish, Ch.B.; Vivek, H.K.; Rai, K.M.L.; Lokanath, N.K., & Kumar, K.A., "Design, synthesis, characterization, and antioxidant activity studies of novel thienyl-pyrazoles"., *Heliyon*, **2021**, *7*(7), e07592. DOI: [10.1016/j.heliyon.2021.e07592](https://doi.org/10.1016/j.heliyon.2021.e07592)
30. Ruzi, Z.; Bozorov, K.; Nie, L.; Zhao, J., & Aisa H.A., "Novel pyrazolo[3,4-d]pyrimidines as potential anticancer agents: Synthesis, VEGFR-2 inhibition, and mechanisms of action panel"., *Biomedicine & Pharmacotherapy*, **2022**, *156*, 113948. DOI: <https://doi.org/10.1016/j.biopha.2022.113948>
31. Alharthy, R.D.; Rashid, F.; Ashraf, A.; Shafiq, Z.; Ford, S.; al-Rashida, M.; Yaqub, M., & Iqbal, J., "Pyrazole derivatives of pyridine and naphthyridine as proapoptotic agents in cervical and breast cancer cells"., *Sci. Rep.*, **2023**, *13*, 5370. DOI: <https://doi.org/10.1038/s41598-023-32489-5>
32. Lan, H.; Song, J.; Yuan, J.; Xing, A.; Zeng D.; Hao, Y.; Zhang, Z.; & Feng, Sh., "Synthesis, Biological Evaluation, DNA Binding, and Molecular Docking of Hybrid 4,6-Dihydrazone Pyrimidine Derivatives as Antitumor Agents"., *Molecules*, **2023**, *28*(1), 187. DOI: [10.3390/molecules28010187](https://doi.org/10.3390/molecules28010187)
34. Sherbiny, F.F.; Ashraf, H.; Bayoumi, El-Morsy, A.M.; Sobhy, M., Hagra, M., "Design, Synthesis, biological Evaluation, and molecular docking studies of novel Pyrazolo[3,4-d]Pyrimidine derivative scaffolds as potent EGFR inhibitors and cell apoptosis inducers"., *Bioorg Chem.*, **2021**, *116*, 105325. DOI: [10.1016/j.bioorg.2021.105325](https://doi.org/10.1016/j.bioorg.2021.105325)
35. Saleh, N.M.; El-gazzar, M.G.; Aly, H.M.; & Othman, R.A., "Novel anticancer fused pyrazole derivatives as EGFR and VEGFR-2 dual TK inhibitors"., *Frontiers in Chemistry*, **2020**, *7*(22), 1-12. DOI: [10.3389/fchem.2019.00917](https://doi.org/10.3389/fchem.2019.00917)
36. Takarada, J.E.; Cunha, M.R.; Almeida, V.M.; Vasconcelos, S.N.S.; Santiago, A.S.; Godoi, P.H.; Salmazo, A.; Ramos, P.Z.; Fala, A.M.; de Souza, L.R.; Da-Silva, I.E.P.; Bengtson, M.H.; Massirer, K.B., & Couñago, R.M., "Discovery of pyrazolo[3,4-d]pyrimidines as novel mitogen-activated protein kinase kinase 3 (MKK3) inhibitors Author links open overlay panel"., *Bioorganic & Medicinal Chemistry*, **2024**, *98*, 117561. DOI: <https://doi.org/10.1016/j.bmc.2023.117561>
37. Maher, M.; Kassab A.E.; Zaher, A.F.; & Mahmoud Z., "Novel pyrazolo[3,4-d]pyrimidines: design, synthesis, anticancer activity, dual EGFR/ErbB2 receptor tyrosine kinases inhibitory activity, effects on cell cycle profile and caspase-3-mediated apoptosis"., *Journal of Enzyme Inhibition and Medicinal Chemistry*, **2019**, *34*(1), 532-546. DOI: [10.1080/14756366.2018.1564046](https://doi.org/10.1080/14756366.2018.1564046)

38. Maher, M.; Kassab, A.E., Zaher, A.F., & Mahmoud, Z., "Novel Pyrazolo[3,4-d]pyrimidines as Potential Cytotoxic Agents: Design, Synthesis, Molecular Docking and CDK2 Inhibition"., *Anticancer Agents Med Chem.*, **2019**, *19*(11), 1368-1381. DOI: 10.2174/1871520619666190417153350
39. Khammas, S.J., & Hamood, A.J., "Synthesis, Cytotoxicity, Xanthine Oxidase Inhibition, Antioxidant of New Pyrazolo{3,4 d}Pyrimidine Derivatives"., *Baghdad Science Journal.*, **2019**, *16*(4), 1003-1009. DOI: [http://dx.doi.org/10.21123/bsj.2019.16.4\(Suppl.\).1003](http://dx.doi.org/10.21123/bsj.2019.16.4(Suppl.).1003)
40. Dong, J.; Zhu, X.; Yu, W.; Hu, X.; Zhang, Y.; Yang, K.; You, Z.; Liu, Z.; Qiao, X., & Song, Y., "Pyrazolo[3,4-d]pyrimidine-based dual HDAC/Topo II inhibitors: Design, synthesis, and biological evaluation as potential antitumor agents"., *Journal of Molecular Structure.*, **2023**, *1272*, 134221. DOI: <https://doi.org/10.1016/j.molstruc.2022.134221>
41. Ali, A.; Banerjee, S.; Kamaal, S.; Usman, M.; Das, N.; Afzal, M.; Alarifi, A.; Sepay, N.; Roy, P., & Ahmad, M., " Ligand substituent effect on the cytotoxicity activity of two new copper(II) complexes bearing 8-hydroxyquinoline derivatives: validated by MTT assay and apoptosis in MCF-7 cancer cell line (human breast cancer)"., *RSC Adv.*, **2021**, *11*(24), 14362-14373. DOI: 10.1039/d1ra00172h
42. Sudhan, S.P.N.; Ahmed, R.N.; Kiyani, H.; & Mansoor, S.Sh., "Ionic liquid 1-butyl-3-methylimidazolium bromide: A green reaction media for the efficient synthesis of 3-methyl-1,4-diphenyl-1,4,5,7-tetrahydro-pyrazolo[3,4-d]pyrimidine-6-ones/thiones using phthalimi de-N-sulfonic acid as catalyst"., *Journal of Saudi Chemical Society.*, **2018**, *22*(3), 269-278. DOI: <http://dx.doi.org/10.1016/j.jscs.2016.07.001>